Available online at www.sciencedirect.com
ScienceDirect
Bioorganic & Medicinal Chemistry 14 (2006) 7880–7892
Bioorganic & Medicinal Chemistry

Synthesis and evaluation of novel 8,5-fused bicyclic peptidomimetic compounds as interleukin-1β converting enzyme (ICE) inhibitors

David L. Soper,[b] Justin X. Sheville,[a] Steven V. O'Neil,[a] Yili Wang,[a] Michael C. Laufersweiler,[a] Kofi A. Oppong,[a] John A. Wos,[a] Christopher D. Ellis,[a] Mark W. Baize,[a] Jack J. Chen,[a] Amy N. Fancher,[a] Wei Lu,[a] Maureen K. Suchanek,[a] Richard L. Wang,[a] William P. Schwecke,[a] Charles A. Cruze,[a] Maria Buchalova,[a] Marina Belkin,[a] Fred Wireko,[c] Amanda Ritter,[c] Biswanath De,[a] Difei Wang[d] and Thomas P. Demuth, Jr.[a,*]

[a]*Procter & Gamble Pharmaceuticals, Inc., 8700 Mason-Montgomery Road, Mason, OH 45040, USA*
[b]*The Procter & Gamble Company, 11510 Reed Hartman Highway, Cincinnati, OH 45241, USA*
[c]*The Procter & Gamble Company, 11810 East Miami River Road, Cincinnati, OH 45252, USA*
[d]*Department of Chemistry and Biochemistry, University of Notre Dame, Notre Dame, IN 46556, USA*

Received 23 June 2006; accepted 26 July 2006

Abstract—An 8,5-fused bicyclic peptidomimetic ring system generated by a stereoselective ring metathesis reaction was elaborated into potent inhibitors of interleukin-1β converting enzyme (ICE, caspase-1). Multiple compounds were found that exhibited ICE IC_{50} values <10 nM and were selective over caspase-3 and caspase-8. These active analogs generally possessed good activity (IC_{50} values <100 nM) in a whole cell assay measuring IL-1β production. Pharmacokinetic analysis of the ethyl acetal prodrug form of a selected active lead revealed a compound with a reasonable plasma half-life (1.1 h) and good oral bioavailability (30%).

1. Introduction

The excessive production of IL-1β contributes to the pathogenesis of acute and chronic inflammatory and autoimmune diseases, including for example, disease progression in rheumatoid arthritis (RA) and osteoarthritis (OA), where it mediates inflammatory symptoms, contributes to the destruction of cartilage proteoglycan, and also induces bone loss in afflicted joints. Other conditions where IL-1β plays a pathogenic role include atherosclerosis, sepsis syndrome, inflammatory bowel syndrome, and periodontal disease.[1] Therefore, intervention in the IL-1 pathway may provide an effective means for the management of inflammatory disorders such as RA.

The caspases are a family of structurally similar, intracellular cysteine proteases primarily responsible for key steps in immunity and the inflammatory response, such as cytokine maturation and apoptosis.[2] Caspase-1 (interleukin-1β converting enzyme, ICE) catalyzes the proteolytic cleavage of the pro-inflammatory cytokines pro-IL-1β and pro-IL-18 to the bioactive forms IL-1β and IL-18.[3] The inhibition of ICE is a recognized target for therapeutic intervention against a variety of chronic inflammatory conditions.

The tetrapeptide **1** (AcYVAD-CHO) was identified as a potent reversible inhibitor of ICE,[4] and was used to demonstrate that inhibition of ICE in whole blood prevented secretion of IL-1β.[5] The X-ray crystal structure of compound **1** bound in the active site of ICE was published and defined key spatial, lipophilic, and hydrogen-bonding interactions for potent ICE inhibition.[6] These are depicted schematically (Fig. 1) and include a lipophilic P4 moiety (the tyrosine side chain), a 'bent' P2–P3 dipeptide central core, a hydrogen-

Keywords: ICE; Caspase-1; Enzyme inhibitor; Interleukin-1β; Cysteine protease; Peptidomimetic compound.
* Corresponding author. Tel.: +1 513 622 0990; fax: +1 866 454 4324; e-mail: demuth.tp@pg.com

0968-0896/$ - see front matter © 2006 Elsevier Ltd. All rights reserved.
doi:10.1016/j.bmc.2006.07.056

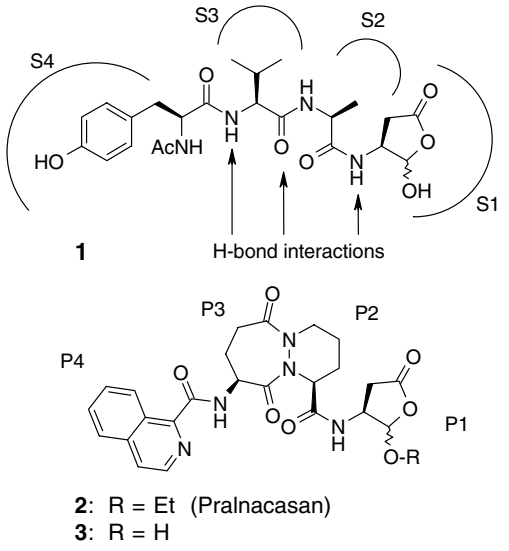

Figure 1. Known ICE inhibitors.

bonding backbone, and an aspartic acid-like cysteine trap.[7]

More recently, rigid peptidomimetic compounds were identified as potent reversible and irreversible inhibitors. Notable among these, Pralnacasan® **2** [8] was characterized as a selective reversible ICE inhibitor which progressed into late stage clinical trials for RA. Pralnacasan® incorporated a bicyclic core to constrain the central dipeptide region of the inhibitor into a preferred conformation that maintained the key hydrogen bond contact points. In addition, a prodrug moiety was used to mask the acidic character of the C-terminal aspartic acid recognition element and allowed the compound to be dosed orally. The lactone acetal prodrug of **2** was reported to undergo enzymatic hydrolysis under physiological conditions to provide the bioactive form of the drug **3**.[9]

We likewise explored P2–P3 constrained systems,[10] and herein we report the synthesis and evaluation of ICE inhibitors based on an 8,5-fused bicyclic scaffold. We believed compounds such as **4** (Scheme 1) would possess the desired conformational constraint for properly orienting the P1 cysteine trap and the hydrophobic P4 residue (R^1), and to allow the key hydrogen-bonding interactions to occur. Inhibitors such as **4** should be readily accessible from the reported bicyclic core **5**.[11] The precursor **5** possessed an ester at the C-terminus which could be hydrolyzed to provide a handle for attachment of the required aspartic acid aldehyde recognition element. Additionally, the nitrogen-terminus of **5** could be deprotected and derivatized to explore the P4 region of our inhibitors.

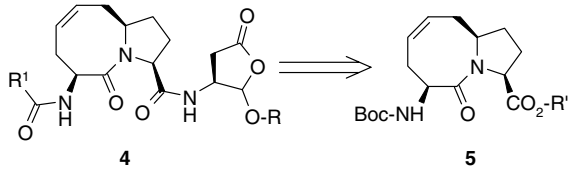

Scheme 1. 8,5-Fused bicyclic ICE inhibitor scaffold.

2. Chemistry

The synthesis of **5** and several diastereomers from intermediate **6** was previously reported, and we elected to follow a similar approach, outlined in Scheme 2. In several steps, L-pyroglutamic acid was converted to an inseparable 3:1 mixture of diastereomeric (5*R*)- and (5*S*)-allyl-(2*S*)-proline ethyl esters **7a** via allylsilane addition to the intermediate methyl aminal **6a**. The mixture was coupled with *N*-Boc-L-allylglycine to yield **8a** as a mixture of isomers. This mixture of isomers **8a** was then subjected to ring-closing olefin metathesis conditions (5–10 mol% 1st generation Grubbs catalyst,[12] reflux, 3 h) resulting in the formation of only one bicyclic product **5a** in 75% yield, resulting from cyclization of the 5*R*-isomer of **8a**. Interestingly, no cyclization of the minor 5*S*-diastereomer of **8a** to the 8,5-bicyclic compound **9a** was observed under these conditions. However, it was previously reported that the precursor **8c**, possessing the 5*S* stereochemistry, was able to cyclize to the metathesis product **9c**, albeit in much lower yield under more forcing conditions (30 mol% catalyst, 116 h).

The related metathesis precursor **8b** likewise provided only the bicyclic product **5b** resulting from cyclization of the major 5*R*-isomer in 70% yield, when subjected to the metathesis reaction. Finally, the inseparable allyl proline mixture **7b** was coupled with *N*-Boc-D-allylglycine, the enantiomer of that used above, and a ~3:1 mixture of 5*R*-**10** and 5*S*-**10** was obtained. When the mixture **10** was treated with 1st generation Grubbs catalyst at 40 °C for 3 h, we observed the formation of a single bicyclic product once again in 21% yield. The identity of the product formed this time was determined to be **12**, resulting from cyclization of the minor 5*S*-proline isomer **10** (84% yield based on 5*S*-**10**). A two dimensional NOESY spectrum was taken to assign the stereochemistry at the ring fusion. A significant NOE was observed between H6 and H10a, indicating that these two protons were on the same face of the 8-membered lactam (Scheme 2). These data were consistent with structure **12** and not **11**.[7] No cyclization of the major isomer 5*R*-**10** was observed under the standard metathesis conditions we employed, in contrast to that previously reported.

We were intrigued by the selectivities observed in the metathesis cyclizations and as a simple probe for the underlying basis of these ring-closing metathesis results, we performed a brief study of the conformational space populations of the substrates 5*R*- and 5*S*-**8b** and 5*R*- and 5*S*-**10** (Fig. 2). These structures were used as simple, all-carbon analogs of the metal carbene complexes involved in the metathesis reaction due to the absence of suitable force field parameters for the metal carbine complexes. It can, however, be expected that they provide suitable representations of the conformational behavior, which is determined by stereocenters remote from the metal. Similar calculations have been used to

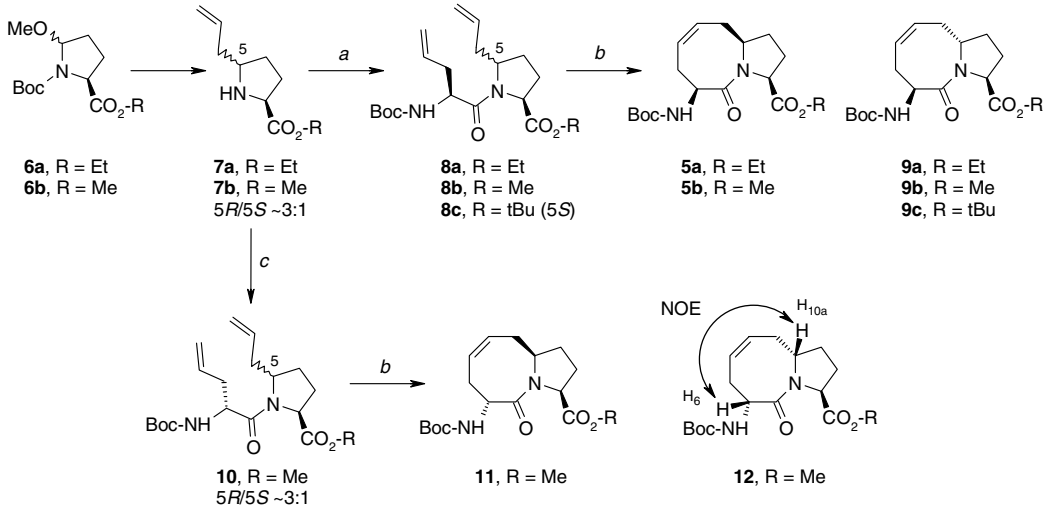

Scheme 2. Reagents and conditions: (a) *N*-Boc-L-allylglycine, DCC, TEA, DMAP, dichloromethane; (b) 5–10% 1st generation Grubbs catalyst, dichloromethane, reflux, 3 h; (c) *N*-Boc-D-allylglycine, DCC, TEA, DMAP, dichloromethane.

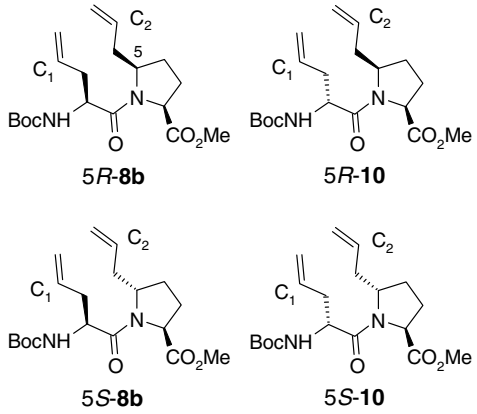

Figure 2. Substrates for ring-closing metathesis reaction.

explain observed RCM results directed at the synthesis of the ingenol ring system.[13]

Through use of a Monte Carlo (MC) search, 8643 and 7639 unique conformers were found for 5*R*-**8b** and 5*S*-**8b**, respectively, while 8927 and 8589 unique conformers were found for 5*R*-**10** and 5*S*-**10**. These findings and the analysis of the convergence of the MC search imply that 50,000-step MC searches are adequate to explore the conformational space populations of the four stereoisomers and to generate a statistically relevant ensemble. Figure 3 shows the conformations within 3 kcal/mol, aligned based on the eight atoms which form the 8-membered ring in the product. In the most stable conformer of 5*R*-**8b**, the distance of C_1–C_2 is about 5.4 Å, while the corresponding distance in 5*S*-**8b** is 5.8 Å. Similarly, the distance of C_1–C_2 in 5*S*-**10** is about 4.9 Å, which is 0.9 Å shorter than that in 5*R*-**10**. It can also be seen that there is relatively little conformational flexibility other than rotation around the vinylic bond in this part of the molecule, resulting in closely related families of conformers. It seems clear from these results that, consistent with the experimental observation, only 5*R*-**8b** and 5*S*-**10** should be able to undergo efficient ring-closing metathesis based on the shorter C_1–C_2 distances.

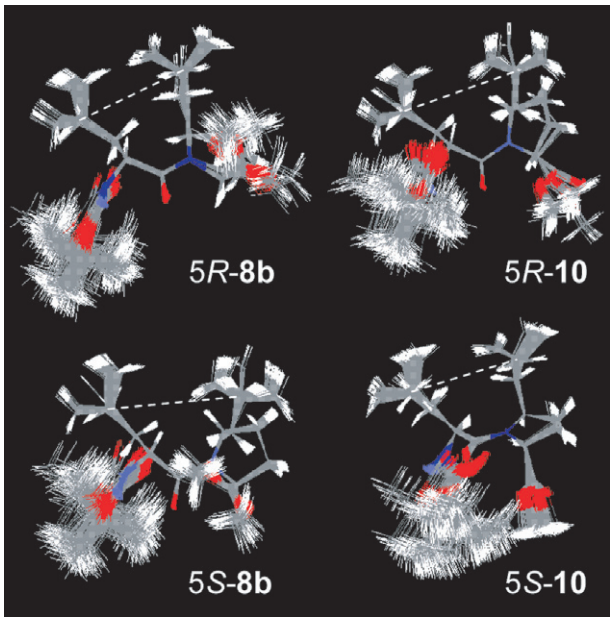

Figure 3. Superimposition of all aligned conformers within 3 kcal/mol range based on the lowest energy conformer for each of the four stereoisomers.

More importantly, this point is found to be true for the overall set of conformations. When the C_1–C_2 distances for all unique conformers of each isomer were plotted against the number of conformations with that distance, it can be seen that only the isomers that have substantial conformational populations in the C_1–C_2 distance range of 3.5–5.5 Å, and especially of 3.5–5.0 Å, can efficiently form the ring-closing metathesis product, as shown as in Figure 4. For example, 5*R*-**8b** does form the 8-membered ring product and has more than 1000 unique conformers possessing a C_1–C_2 distance from 3.5 to 5.0 Å; however, 5*S*-**8b**, which has less than 200 unique con-

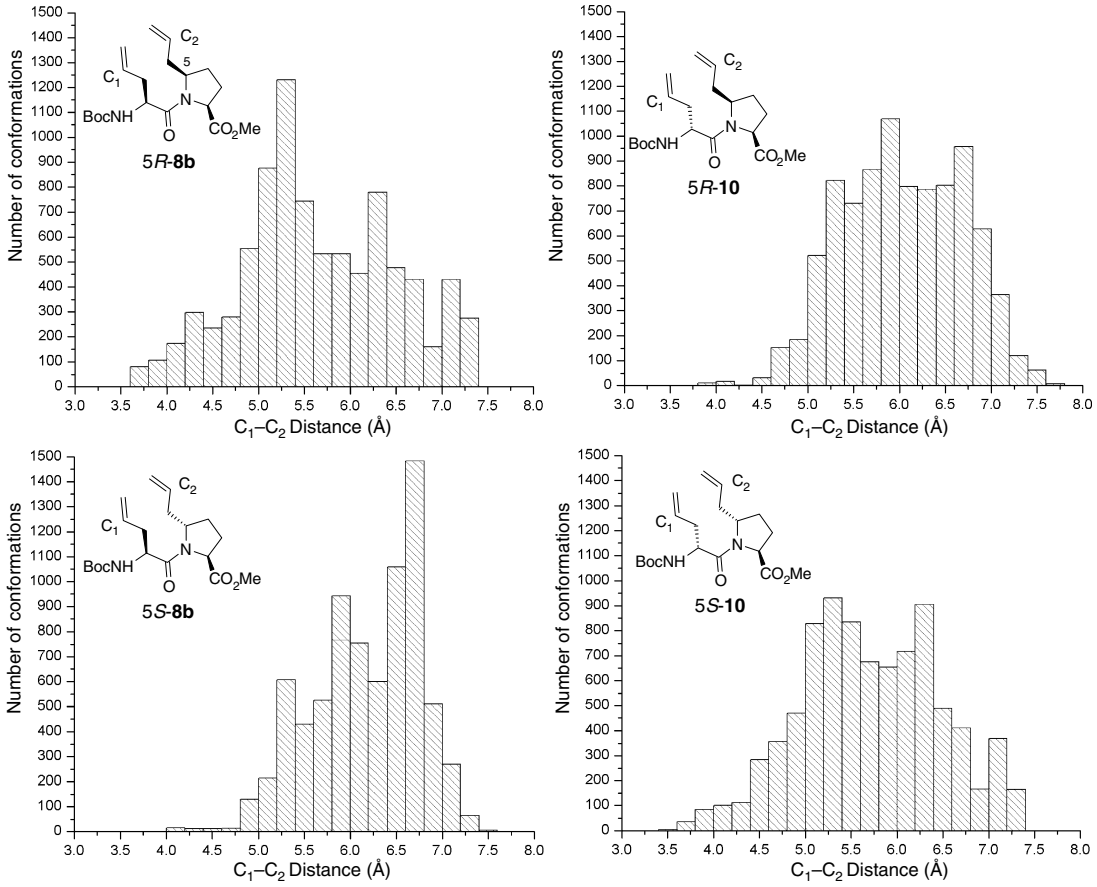

Figure 4. C_1–C_2 distances (in angstroms) versus number of conformations of the four stereoisomers.

formers in the same range, does not undergo ring-closure using the standard reaction conditions. The calculated results agree with the experimental results very well, and this simple computational tool could be used as a qualitative basis to predict ring-closure potential for other similar compounds.

Although these calculated results are in good agreement with the experimental findings and provide a reasonable rationale for them, this study of the substrates themselves is not as appropriate as a corresponding study of the substrate-derived ruthenium carbene complexes that serve as the key intermediates in the cyclization reaction. However, this more rigorous approach is beyond the scope of the present work, especially due to the lack of appropriate parameter sets for these intermediates. Also, Curtin–Hammett considerations may argue against the validity of this analysis.[14] However, there are clear trends for the population of energetically accessible conformations that are required for cyclization to occur, with quite notable differences being seen among the reacting and non-reacting diastereomers. These differences could translate into increased strain energy in the cyclization transition states for the non-reacting diastereomers, thus leading to much slower rates of cyclization for these compounds compared to the diastereomers that do participate in the ring-closing metatheses. To be completely valid, the consideration of Curtin–Hammett factors would require a much more rigorous investigation of both ground state and transition state energies.

Once the bicyclic core **5** had been synthesized on sufficient scale for elaboration into potential ICE inhibitors, the Boc-protecting group was removed by treatment of **5** with thionyl chloride in methanol (Scheme 3). The hydrochloride salt was neutralized with triethylamine and treated with aryl acid chlorides or carbodiimide coupling reagents with the aryl carboxylic acids to give **13**. Compound **13f** (saturated 8,5-ring system, $R = m$-chlorophenyl) was subjected to X-ray structure determination to confirm the stereochemical assignment in the bicyclic scaffold. Figure 5 depicts the results from the crystal structure determination and confirms the stereochemical assignment as previously described. Compound **13** was then hydrolyzed with lithium hydroxide to give the free carboxylic acid **14**. The coupling of an aspartic acid aldehyde synthon was then carried out via one of two separate routes.

The first route investigated was one that utilized compound **21**.[15] The alloc-protecting group of **21** was removed in situ with $Pd(Ph_3P)_4$ and dimethylbarbituric acid in CH_2Cl_2 at room temperature for 10 min, at which time, compound **14** was added in DMF followed immediately by HOBt and EDAC. The coupling was typically completed in 2 h, but isolation of pure compound **16** was generally difficult due to contamination

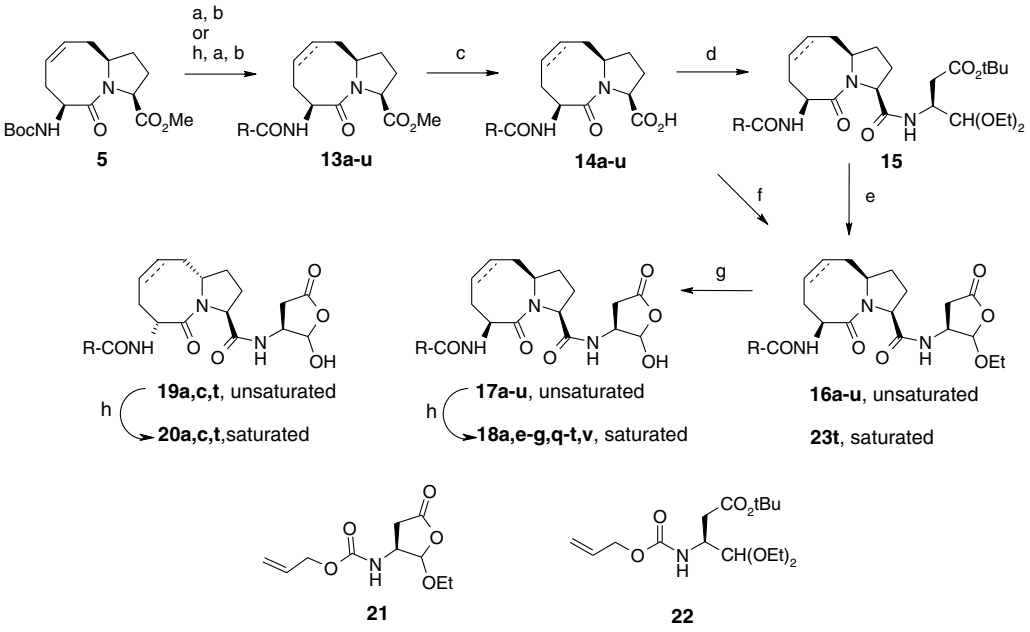

Scheme 3. Reagents and conditions: (a) $SOCl_2$, MeOH, 100%; (b) TEA, aryl acid chloride, CH_2Cl_2, 18 h, 80–95%; or EDAC, HOBt, aryl acid, TEA, 18 h, 70–95%; (c) LiOH, THF/H_2O (3:1), 95%; (d) compound **22** 85–95%; (e) TFA, CH_2Cl_2, 80–95%; (f) compound **21**, *N*,*N*-dimethylbarbituric acid, $(Ph_3P)_4Pd$, CH_2Cl_2, HOBt, EDAC, 40–80%; (g) TFA, CH_3CN, H_2O, 60–95%; (h) H_2, 10% Pd/C, 100%.

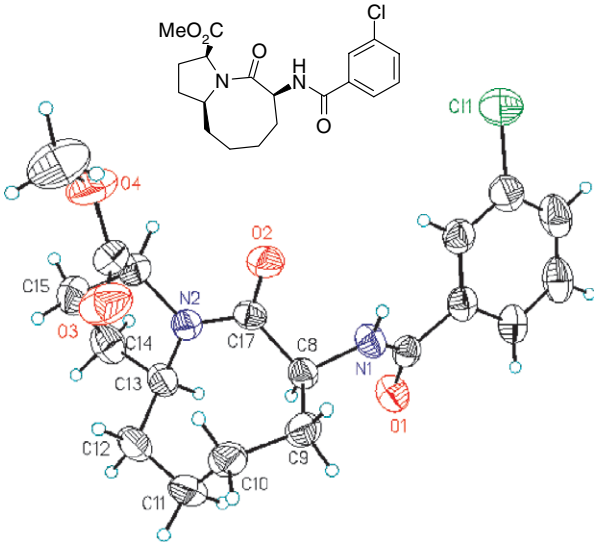

Figure 5. Single crystal X-ray structure determination of compound **13f** (saturated 8,5-ring system).[16]

of the product with Ph_3PO. Consequently, crude **16** was hydrolyzed with TFA in CH_3CN/H_2O to obtain the final inhibitors **17**. In the second route, intermediate **22** was used in the coupling reaction in place of **21**. Using the same coupling conditions described above, compound **15** was obtained in excellent yields (85–95%). In this approach, compound **15** was isolated with purities of >98% following flash chromatography on silica gel. Treatment of **15** with trifluoroacetic acid in anhydrous dichloromethane for 10 min gave **16** in a >95% yield. This route allowed for the production of substantial quantities of a prodrug form analogous to Pralnacasan® (**2**) in high yield and purity for pharmacokinetic studies.

Lastly, saturated analogs (**18**) were synthesized by either hydrogenation of intermediate **5** prior to elaboration or hydrogenation of final inhibitors **17**. Diastereomeric inhibitors (**19** and **20**), possessing inverted stereocenters at the ring fusion and the P3 amine, were also synthesized via an identical sequence starting from intermediate **12**.

3. Results and discussion

A series of potential ICE inhibitors based on the 8,5-bicyclic scaffold were synthesized wherein the substituent R (in structure **17**) was varied to introduce hydrophobic groups into the P4 region of the inhibitor (Table 1). The compounds were evaluated for their potency at inhibiting ICE (caspase-1) and for their selectivity against inhibiting the related caspase-3 and caspase-8. In addition, the compounds were tested in the THP-1 whole cell assay measuring the inhibition of IL-1β production caused by exposure to the ICE inhibitor.

Compound **17a** (R = phenyl) was potent against ICE enzyme (IC_{50} 23 nM), but showed poor activity in the THP-1 whole cell assay (IC_{50} > 1000 nM). Substitution on the phenyl (**17b**–**17p**) resulted in modest variations in the ICE enzyme potency, with a slight preference for hydrophobic substituents at the *meta*-position. In contrast, most of the phenyl substitutions showed increases in the whole cell potency (THP-1 IC_{50}). Overall, *para*-substitution generally led to a reduction in whole cell activity. The bicyclic aryl compounds (**17q**–**17t**) showed excellent enzyme activity, all having IC_{50} < 10 nM. Except for the benzothiophene derivative **17q**, the THP-1 data for these compounds also showed increased potency, especially with **17r** and **17s** having

Table 1. In vitro enzyme inhibition and whole cell THP-1 IC_{50} data for compounds **17**–**20**

Compound	R	Enzyme IC_{50}[a] (nM)			Whole cell IC_{50}[b] (nM) THP-1
		ICE	Caspase-3	Caspase-8	
3[c]	—	3.6	1300	40	190
17a	Phenyl	23	$>10^4$	1400	1100
17b	2-Methoxyphenyl	140	$>10^4$	4100	110
17c	3-Methoxyphenyl	15	$>10^4$	2300	90
17d	4-Methoxyphenyl	32	$>10^4$	2400	170
17e	2-Chlorophenyl	50	$>10^4$	610	330
17f	3-Chlorophenyl	23	$>10^4$	2900	200
17g	4-Chlorophenyl	49	$>10^4$	4200	710
17h	2-Methylphenyl	16	$>10^4$	320	450
17i	3-Methylphenyl	13	$>10^4$	800	210
17j	4-Methylphenyl	170	$>10^4$	>100	1800
17k	2-Fluorophenyl	35	$>10^4$	1100	560
17l	3-Fluorophenyl	18	$>10^4$	690	380
17m	4-Fluorophenyl	13	$>10^4$	480	100
17n	2-Trifluoromethylphenyl	23	$>10^4$	380	270
17o	3-Trifluoromethylphenyl	7	$>10^4$	2900	440
17p	4-Trifluoromethylphenyl	32	$>10^4$	420	2500
17q	2-Benzothiophene	7.0	$>10^4$	2600	1100
17r	1-Naphthyl	4.2	$>10^4$	380	17
17s	2-Naphthyl	2.8	$>10^4$	2000	52
17t	1-Isoquinolyl	3.3	$>10^4$	960	190
17u	Cinnamyl	69	$>10^4$	8200	110
18a	Phenyl	6.3	$>10^4$	540	1100
18e	2-Chlorophenyl	8.5	8400	41	150
18f	3-Chlorophenyl	2.6	$>10^4$	210	390
18g	4-Chlorophenyl	5.3	$>10^4$	250	nt
18q	2-Benzothiophene	3.3	$>10^4$	810	480
18r	1-Naphthyl	1	$>10^4$	66	3
18s	2-Naphthyl	<1	$>10^4$	390	32
18t	1-Isoquinolyl	<1	$>10^4$	160	54
18v	2,6-Dimethylphenyl	56	8600	37	560
19a	Phenyl	3900	$>10^4$	$>10^4$	$>10^4$
19c	3-Methoxyphenyl	3700	$>10^4$	$>10^4$	$>10^4$
19t	1-Isoquinoyl	1200	$>10^4$	$>10^4$	$>10^4$
20a	Phenyl	410	$>10^4$	$>10^4$	$>10^4$
20c	3-Methoxyphenyl	590	$>10^4$	$>10^4$	$>10^4$
20t	1-Isoquinoyl	880	$>10^4$	$>10^4$	$>10^4$

[a] Enzyme IC_{50} results are expressed as ±30% or less.
[b] Whole cell THP-1 IC_{50} results varied approximately ±2-fold.
[c] Pralnacasan free drug.

IC_{50} < 100 nM. The cinnamyl derivative **17u** (a bicyclic mimetic) also showed very good whole cell potency in the THP-1 assay.

Molecular modeling was used to predict a binding mode for the 8,5-fused bicyclic inhibitors to the active site of ICE, and to provide a comparison to the published X-ray crystallographic structure of compound **1** (AcYVAD-CHO) complexed to ICE (Fig. 6a). Based on the single crystal X-ray structure of **13f** (saturated 8,5-ring system, R = *m*-chlorophenyl), a model of inhibitor **18f** was constructed. The rotatable bonds of the P1 and P4 moieties of the model were oriented in low energy conformations that overlapped with the corresponding P1 and P4 substituents in the AcYVAD-CHO structure from the crystal structure. Finally, this model was docked into the active site of the ICE protein crystal structure in place of the AcYVAD-CHO structure (Fig. 6b). Based on this model, the proline portion of the 8,5-bicyclic ring was seen to fit into S2 pocket, and the 8-membered ring occupied the S3 pocket analogously to the Val side chain in the tetrapeptide inhibitor. In addition, key hydrogen bond interactions were maintained by **18f**, analogous to the AcYVAD-CHO structure. Finally, both the P1 aspartyl moiety and P4 substituent were appropriately displayed to maximize their interactions with their respective binding sites. Overall, the molecular model with compound **18f** was consistent with the binding mode of AcYVAD-CHO observed in the ICE crystal structure.

To establish that our compounds were selectively inhibiting ICE (caspase-1) over other caspases, we screened against caspase-3 and caspase-8. Selectivity over caspase-3 was consistent with most compounds showing >10 μM inhibition. In addition, most compounds showed >50-fold selectivity against caspase-8. Interestingly, several of the compounds with *ortho*-substituted aryl groups as the P4 moiety showed improved activity against caspase-8. In fact, the 2,6-dimethylphenyl-

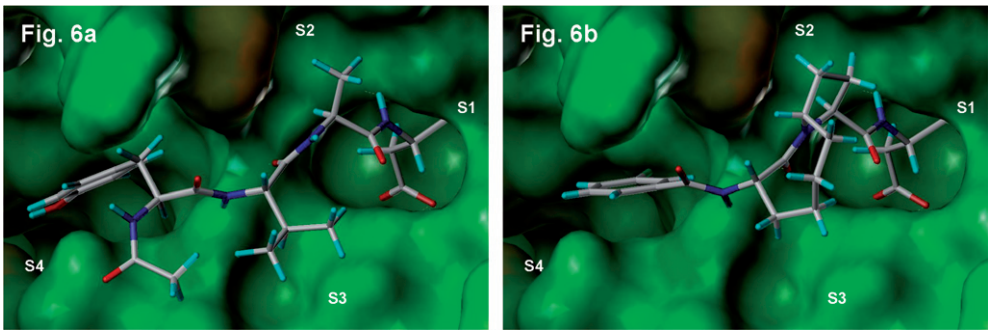

Figure 6. (a) X-ray structure of AcYVAD-CHO complexed to ICE[6]; (b) molecular model of compound **18f** complexed to ICE.

Table 2. Pharmacokinetic analysis, oral bioavailability, and plasma stability of selected compounds

Compound	Ethyl prodrug	$t_{1/2}$[a] (h)	% F[a] (rat)	Plasma stability $t_{1/2}$[b] (h)
17s	No	2.2	1	Not tested
23t	Yes	1.1	30	0.2

[a] Values are based on the amount of free drug measured in the plasma.
[b] Data are expressed as the half-life for disappearance of prodrug as determined by reverse phase HPLC.

substituted analog **18v** was a dual caspase inhibitor, exhibiting comparable potency at inhibiting ICE and caspase-8 (IC_{50} values <100 nM).

Several of the 8,5-bicyclic ICE inhibitors which were potent in the enzyme and THP-1 assays, and which maintained selectivity versus caspase-3 and -8, were further characterized in vitro and in vivo. Consistent with results previously described for peptidomimetic ICE inhibitors, the 8,5-bicyclic compounds (analogs **17** and **18**) showed generally low oral bioavailability in pharmacokinetic studies using rats. For example, compound **17s** exhibited only a 1% oral bioavailability, although it had a reasonable plasma half-life of 2.1 h (Table 2).

A prodrug strategy was therefore employed to improve the oral bioavailability of selected ICE inhibitors. For example, compound **23t** (the ethyl acetal prodrug of compound **18t**) was identified as one of the better performing analogs in a preliminary PK study,[17] exhibiting good oral bioavailability (30%, measured as free drug) and a plasma half-life of the corresponding free drug of 1.1 h. The prodrug **23t** proved short-lived in plasma and released the corresponding free drug with a half-life <15 min. After oral administration, no prodrug was observed in rat plasma, and only free drug (e.g., **18t**) was detected. Overall, the ethyl acetal prodrug approach was variably successful in improving the oral bioavailability of other 8,5-bicyclic ICE inhibitors, possibly as a result of the prodrugs' reduced aqueous solubility and their differing stability profiles (data not shown).

4. Conclusion

We described a stereoselective synthesis of an 8,5-bicyclic peptidomimetic scaffold using a ring-closing metathesis approach. A molecular modeling study using a Monte Carlo based conformational search provided calculated results that were in good agreement with the experimental cyclization findings and provided a reasonable rationale for them. We further elaborated the 8,5-bicylic scaffold and established that this scaffold produced potent ICE inhibitors. Based on single crystal X-ray data and molecular modeling, we believe that the bicyclic ring system allowed for the proper display of functionality at the P4 and P1 positions while maintaining key hydrogen bonds in the ICE enzyme active site. Numerous compounds were found with good ICE inhibition (<10 nM), good selectivity versus caspase-3 and caspase-8, and whole cell potency (<100 nM) that were comparable or superior to the reference inhibitor **3**. Good pharmacokinetic performance was achieved with the ethyl acetal prodrug **23t** of one of the better ICE inhibitors (**18t**), exhibiting 30% oral bioavailability and a 1.1 h half-life in rats. Overall, these results suggest that further in vivo evaluation of selected compounds in this class is warranted.

5. Experimental

5.1. General

^{1}H NMR spectra were recorded on a Varian Unity Plus 300 MHz spectrometer and are referenced to either the deuteriochloroform singlet at 7.27 ppm or deuteriomethanol singlet at 4.87 ppm. ^{13}C spectra were recorded on a Varian Unity Plus 300 MHz spectrometer and are referenced to either the centerline of the deuteriochloroform triplet at 77.0 ppm or the deuteriomethanol heptet at 49.2 ppm. Mass spectra were obtained on either a Fison Platform-II Quadrapole Mass Spectrometer or a Fison Trio2000 Quadrapole Mass Spectrometer. High-resolution mass spectra were obtained on a Micromass LCT Time-of-Flight Mass Spectrometer. All solvents were purchased anhydrous (Aldrich Chemical) and used without further purification. All air-sensitive reactions were performed under an anhydrous nitrogen atmosphere. Flash chromatography was performed on silica gel (70–230 mesh; Aldrich). Thin-layer chromatography analysis was performed on glass mounted silica gel plates (250 μm Analtech) and visualized using UV, iodine, or potassium permanganate in 5% aqueous NaOH.

5.2. Inhibition of ICE, caspase-3, and caspase-8 enzymes

The isolated enzyme (ICE, caspase-3, and caspase-8) assays were performed in a 96-well format using fluorogenic substrates, enzymes and control peptide inhibitors purchased from BioMol Research Laboratories (Plymouth Meeting, PA). The assay was conducted according to the manufacturer's instructions. Enzyme inhibition was monitored over 30 min at 37 °C by measuring fluorescence using a BMG Fluostar plate reader (excitation filter 390 nm, emission filter 460 nm). IC_{50} values were calculated based on the equation $IC_{50} = [I]/(V_o/V_i) - 1$, where V_i is the initial velocity of substrate cleavage in the presence of inhibitor at concentration [I] and V_o is the initial velocity in the absence of inhibitor.

5.3. Inhibition of IL-1β production in a cell-based assay

A suspension of human monocytic cells (THP-1, ATCC strain TIB202, 2×10^6/mL in RPMI 1640 medium from Gibco-BRL) was plated in 96-well plates, incubated with or without compounds (administered as solutions in DMSO, such that test concentrations ranged from 1 nM to 10 μM) for 15 min, and then stimulated with LPS (1 μg/mL) for a total of 4 h. Cells were centrifuged and the conditioned media were collected to quantify the release of IL-1β by an ELISA measurement according to the manufacturer's instructions (R&D Systems, catalog no. DLB50) or stored at −20 °C for future use.

5.4. Pharmacokinetic analysis and oral bioavailability

Preliminary pharmacokinetic studies were conducted utilizing male Sprague–Dawley rats approximately 8–12 weeks old and weighing 225–300 g. A 40% hydroxypropyl-β-cyclodextrin solution containing test compound was administered at the dose level of 30 mg/kg and volume of 10 mL/kg to two animals via oral gavage. Blood samples were collected using the Culex automated blood collection system at time points: 0, 0.5, 1, 2, 4, 6, 8, 12, and 24 h. The blood samples were processed and the plasma frozen at −75 °C until analyzed. A pharmacokinetic analysis of the plasma concentration–time data was conducted using non-compartmental techniques.

5.5. Computational methodology

A 50,000-step Monte Carlo search for conformations of the four substrates (5*R*-**8b**, 5*S*-**8b**, 5*R*-**10**, and 5S-**10**) was performed using the Merck Molecular Force Field (MMFF)[18] as implemented in the MacroModel 7.0 package.[19] The MMFF was parameterized by a large set of quantum chemical calculations of common organic structures at the HF/6-31G* level, and it was tested extensively on a variety of small organic molecules. Solvation effects for chloroform were included via the Generalized Born/Surface Area Continuum model (GB/SA),[20] as implemented in MacroModel 7.0. The GB/SA model has been tested to calculate the absolute free energies of hydration with a high degree of accuracy. Only structures within 50 kJ/mol of the global minimum were stored and the full dataset was used for the statistical analysis.

5.6. Synthesis

5.6.1. Methyl (3*S*,6*S*,8*Z*,10a*R*)-6-[(isoquinolin-1-ylcarbonyl)amino]-5-oxo-1,2,3,5,6,7,10,10a-octahydropyrrolo-[1,2-*a*]azocine-3-carboxylate (13t). Methyl (3*S*,6*S*,8*Z*,10a*R*)-6-[(*tert*-butoxycarbonyl)-amino]-5-oxo-1,2,3,5,6,7,10,10a-octahydropyrrolo[1,2-*a*]azocine-3-carboxylate **5** (3.46 g, 10.2 mmol) was treated with 1.5 mL of thionyl chloride in 50 mL of methanol for 2 h at room temperature. The solvent was removed under reduced pressure leaving 2.43 g (100%) of crude product as an orange crystal. The deprotected amine (1.69 g, 7.1 mmol) and 1-isoquinolinic acid (2.46 g, 14.2 mmol) were dissolved in 75 mL of dichloromethane. To this solution were added dimethylaminopyridine (0.87 g, 7.1 mmol) and dicyclohexylcarbodiimide (2.93 g, 14.2 mmol). The reaction mixture was stirred overnight, during which time a precipitate formed. The solid was filtered and washed with dichloromethane. The filtrate was reduced to dryness and taken up in ether. Additional precipitates formed and were removed by filtration. The filtrate was again reduced to dryness. The residue was chromatographed on a silica gel column (50% ethyl acetate/hexanes), giving compound **13t** as an oil (1.62 g, 58%). ^{1}H NMR ($CDCl_3$): δ 9.55 (m, 1H), 9.18 (d, J = 7.3 Hz, 1H), 8.50 (d, J = 5.5 Hz, 1H), 7.88–7.65 (m, 4H), 5.99–5.81 (m, 2H), 5.38 (m, 1H), 4.59 (dd, J = 8.7, 3.2 Hz, 1H), 4.26 (m, 1H), 3.76 (s, 3H), 3.03–2.86 (m, 2H), 2.60–2.50 (m, 2H), 2.23–1.98 (m, 4H). ^{13}C NMR ($CDCl_3$): δ 172.7, 170.9, 165.7, 148.1, 140.8, 137.6, 130.6, 129.6, 128.7, 127.7, 127.2, 127.1, 126.4, 124.5, 60.5, 59.1, 52.3, 51.3, 35.1, 33.4, 27.5. ESI-MS 394.14 (M+H).

5.6.2. (3*S*,6*S*,8*Z*,10a*R*)-6-[(Isoquinolin-1-yl-carbonyl)-amino]-5-oxo-1,2,3,5,6,7,10,10a-octahydropyrrolo[1,2-*a*]azocine-3-carboxylic acid (14t). Compound **13t** (1.62 g, 4.1 mmol) was added to 20 mL of 3:1 tetrahydrofuran/water. Lithium hydroxide (0.25 g, 5.9 mmol) was added and the reaction mixture was stirred for 18 h. Ethyl acetate was added and the organics were sequentially washed with 1 N HCl and brine, and then dried over magnesium sulfate. Solvent was evaporated leaving **14t** an oil (1.41 g, 90%), which was used without further purification. ^{1}H NMR ($CDCl_3$): δ 9.30 (d, J = 8.5 Hz, 1H), 8.92 (d, J = 7.7 Hz, 1H), 8.53 (d, J = 7.8 Hz, 1H), 7.93 (m, 2H), 7.83–7.71 (m, 2H), 5.88 (m, 1H), 5.75 (m, 1H), 5.50 (m, 1H), 4.70 (d, J = 7.4 Hz, 1H), 4.37 (m, 1H), 3.10–2.91 (m, 2H), 2.44 (m, 3H), 2.21 (m, 1H), 2.03 (m, 2H). HRMS calcd for $C_{21}H_{22}N_3O_4$ 380.1610, found 380.1610.

5.6.3. (3*S*,6*S*,8*Z*,10a*R*)-*N*-[(3*S*)-2-Ethoxy-5-oxotetrahydro-furan-3-yl]-6-[(isoquinolin-1-ylcarbonyl)-amino]-5-oxo-1,2,3,5,6,7,10,10a-octahydro-pyrrolo[1,2-*a*]azocine-3-carboxamide (16t). To a solution of allyl [(3*S*)-2-ethoxy-5-oxotetrahydrofuran-3-yl]carbamate **21** (1.83 g, 8.0 mmol) in dichloromethane (30 mL) were added *N*,*N*-dimethylbarbituric acid (2.98 g, 47.8 mmol) and tetrakispalladium(0) triphenylphosphine (0.85 g, 0.07 mmol). The

resulting mixture bubbled and was allowed to stir at room temperature for 15 min. To this mixture were added compound **14t** (1.2 g, 3.15 mmol), hydroxybenztriazole (1.0 g, 18.5 mmol) and 1-(3-dimethylaminopropyl)-3-ethyl carbodiimide hydrochloride (1.4 g, 18.5 mmol). The reaction mixture was allowed to stir for 2 h at room temperature. The reaction mixture was then poured into water and extracted with ethyl acetate. The organic layers were washed with saturated sodium bicarbonate, brine, dried with sodium sulfate, and concentrated in vacuo. Silica gel chromatography (ethyl acetate) afforded **16t** as a yellow foam (1.42 g, 89%). ^{1}H NMR ($CDCl_3$): δ 9.50 (m, 1H), 9.02 (d, J = 7.7 Hz, 1H), 8.50 (d, J = 5.4 Hz, 1H), 7.83 (m, 3H), 7.69–7.41 (m, 3H), 5.84 (m, 1H), 5.70 (m, 1H), 5.49 (m, 2H), 4.71 (m, 2H), 4.26 (m, 1H), 3.90 (m, 1H), 3.71 (m, 1H), 3.17–2.95 (m, 2H), 2.80 (m, 1H), 2.51–2.30 (m, 4H), 2.14 (m, 1H), 1.90 (m, 2H), 1.31 (t, J = 7.0 Hz, 3H). HRMS calcd for $C_{28}H_{32}N_3O_6$ 506.2291, found 506.2285.

5.6.4. Alternative coupling method: (3*S*,6*S*,10a*S*)-*N*-[(3*S*)-2-Ethoxy-5-oxotetrahydrofuran-3-yl]-6-[(isoquinolin-1-ylcarbonyl)amino]-5-oxo-decahydro-pyrrolo[1,2-*a*]azocine-3-carboxamide (23t). To a solution of *tert*-butyl allyloxy)carbonyl]-amino}-4,4-diethoxybutanoate **22** (18.9 g, 57.3 mmol) in dichloromethane (200 mL) were added *N*,*N*-dimethylbarbituric acid (14.35 g, 92.0 mmol) and tetrakispalladium(0) triphenylphosphine (2.0 g, 1.7 mmol). The resulting mixture bubbled and was allowed to stir at room temperature for 15 min. To this mixture were added (3*S*,6*S*,10a*S*)-6-[(isoquinolin-1-yl-carbonyl)amino]-5-oxodecahydropyrrolo[1,2-*a*]-azocine- 3-carboxylic acid (14.0 g, 36.8 mmol, prepared by catalytic hydrogenation of **14t** using 10% palladium on carbon), hydroxybenztriazole (8.0 g, 59.3 mmol), and 1-(3-dimethylaminopropyl)-3-ethyl carbodiimide hydrochloride (11.31 g, 59.0 mmol). The reaction mixture was allowed to stir for 1 h at room temperature. The reaction mixture was then poured into water and extracted with ethyl acetate. The organic layers were sequentially washed with saturated sodium bicarbonate and brine, then dried with magnesium sulfate, and concentrated in vacuo. Silica gel chromatography (50% ethyl acetate/hexanes) afforded *tert*-butyl (3*S*)-4,4-diethoxy-3-[({(3*S*,6*S*,10a*S*)-6-[(isoquinolin-1-yl-carbonyl)amino]-5-oxodecahydropyrrolo[1,2-*a*]azocin-3-yl}carbonyl)amino]butanoate as a yellow foam (21.2 g, 94% yield). ^{1}H NMR ($CDCl_3$): δ 9.56 (dd, J = 8.4, 1.2 Hz, 1H), 9.02 (d, J = 7.8 Hz, 1H), 8.53 (d, J = 5.4 Hz, 1H), 7.87 (d, J = 8.1 Hz, 1H), 7.81 (d, J = 5.7 Hz, 1H), 7.72 (m, 2H), 7.05 (d, J = 9.0 Hz, 1H), 5.23 (m, 1H), 4.60 (d, J = 4.2 Hz, 1H), 4.56 (d, J = 7.2 Hz, 1H), 4.49–4.35 (m, 2H) 3.74 (m, 3H), 3.58 (m, 3H), 2.59 (d, J = 5.7 Hz, 2H), 2.41 (m, 1H), 2.27–2.01 (m, 3H), 1.93–1.70 (m, 8H), 1.42 (s, 9H), 1.19 (t, J = 6.0 Hz, 6H). HRMS calcd for $C_{33}H_{47}N_4O_7$ 611.3436, found 611.3445.

tert-Butyl (3*S*)-4,4-diethoxy-3-[({(3*S*,6*S*,10a*S*)-6-[(isoquinolin-1-ylcarbonyl)amino]-5-oxodecahydropyrrolo-[1,2-*a*]azocin-3-yl}carbonyl)amino]butanoate (21.2 g, 34.8 mmol) in approximately 200 mL anhydrous dichloromethane was treated with 20 mL of TFA and stirred for 10 min. The solvent was removed and 20 mL of dichloromethane followed by 80 mL of toluene was added. Again the solvent was removed. The residue was chromatographed on silica gel (80% ethyl acetate/hexanes) giving 17.4 g (98% yield) of **23t** as a pale yellow solid. ^{1}H NMR ($CDCl_3$): δ 9.50 (t, J = 8.7 Hz, 1H), 8.92 (dd, J = 29.4 Hz, 7.5, 1H), 8.52 (d, J = 5.4 Hz, 1H), 7.90–7.34 (m, 5H), 5.51 (d, J = 5.4 Hz, 0.5H), 5.40 (s, 0.5H), 5.20 (m, 1H), 4.71 (m, 0.5H), 4.58 (dt, J = 24.0, 7.8 Hz, 1H), 4.38 (m, 1.5H), 3.99–3.83 (m, 2H), 3.76–3.63 (m, 2H), 2.96 (m, 1H), 2.50 (m, 1H), 2.44 (m, 1H), 1.78 (m, 8H), 1.30 (dt, J = 18.0, 6.9 Hz, 3H). ^{13}C NMR ($CDCl_3$): δ 175.2, 173.9, 172.2, 172.1, 171.9, 165.6, 148.2, 140.6, 137.6, 130.7, 128.9, 127.7, 127.1, 124.7, 107.2, 101.4, 65.9, 65.6, 60.8, 59.9, 59.7, 52.6, 50.4, 50.2, 48.6, 37.2, 36.8, 36.0, 35.8, 33.6, 32.9, 32.6, 32.4, 28.1, 25.7, 23.5, 23.4, 15.1. HRMS calcd for $C_{27}H_{33}N_4O_6$ 509.2400, found 509.2395.

5.6.5. (3*S*,6*S*,8*Z*,10a*R*)-*N*-[(3*S*)-2-Hydroxy-5-oxotetrahydrofuran-3-yl]-6-[(isoquinolin-1-ylcarbonyl)-amino]-5-oxo-1,2,3,5,6,7,10,10a-octahydropyrrolo[1,2-*a*]azocine-3-carboxamide (17t). (3*S*,6*S*,8*Z*,10a*R*)-*N*-[(3*S*)-2-Ethoxy-5-oxotetrahydro-furan-3-yl]-6-[(isoquinolin-1-ylcarbonyl)amino]-5-oxo-1,2,3,5,6,7,10,10a-octahydropyrrolo[1,2-*a*]azocine-3-carboxamide **16t** (1.42 g, 2.80 mmol) was stirred in a solution of 5 mL trifluoroacetic acid, 5 mL acetonitrile, and 2.5 mL water for 2 h. Solvents were removed and the residue was taken up twice in ethyl acetate and evaporated to remove excess TFA. The oil was then chromatographed on silica gel with ethyl acetate containing 0.1% acetic acid, yielding **17t** as a yellow foam (1.18 g, 78.4%). ^{1}H NMR ($CDCl_3$): δ 9.30 (m, 1H), 8.85 (d, J = 7.6 Hz, 1H), 8.48 (d, J = 5.4 Hz, 1H), 7.87–7.34 (m, 6H), 5.92–5.71 (m, 3H), 5.54 (m, 1H), 4.71–4.35 (m, 3H), 3.03 (m, 4H), 2.43 (m, 3H), 2.19 (m, 2H), 1.98 (m, 1H). ^{13}C NMR (CDCl3): δ 173.9, 172.5, 171.4, 165.9, 147.9, 140.7, 137.6, 131.4, 130.8, 128.9, 127.5, 127.2, 125.6, 124.9, 61.7, 59.1, 50.4, 34.2, 33.4, 32.3, 27.0. HRMS calcd for $C_{25}H_{27}N_4O_6$ 479.1931, found 479.1934.

5.6.6. (3*S*,6*S*,10a*S*)-*N*-[(3*S*)-2-Hydroxy-5-oxotetrahydrofuran-3-yl]-6-[(isoquinolin-1-ylcarbonyl)-amino]-5-oxo-decahydropyrrolo[1,2-*a*]azocine-3-carboxamide (18t). (3*S*,6*S*,8*Z*,10a*R*)-*N*-[(3*S*)-2-hydroxy-5-oxotetrahydrofuran-3-yl]-6-[(isoquinolin-1-ylcarbonyl)amino]-5-oxo-1,2,3,5,6,7,10,10a-octahydro-pyrrolo[1,2-*a*]azocine-3-carboxamide **17t** (75 mg, 0.15 mmol) was stirred under a balloon of hydrogen with 20 mg of 5% palladium on carbon in ethyl acetate. After 2 h the solution was filtered through a syringe filter and solvent was evaporated to obtain 69 mg of **18t** (91%) as a white foam. ^{1}H NMR ($CDCl_3$): δ 9.37 (m, 1H), 8.78 (m, 1H), 8.47 (m, 1H), 7.88–7.66 (m, 4H), 5.86 (m, 1H), 5.18 (m, 1H), 4.60–4.25 (m, 5H), 2.98–2.45 (m, 2H), 2.23–1.71 (m, 12H). HRMS calcd for $C_{25}H_{29}N_4O_6$ 481.2087, found 481.2074.

5.6.7. (3*S*,6*S*,8*Z*,10a*R*)-6-(Benzoylamino)-*N*-[(3*S*)-2-hydroxy-5-oxotetrahydrofuran-3-yl]-5-oxo-1,2,3,5,6,7,10,10a-octahydropyrrolo[1,2-*a*]azocine-3-carboxamide (17a). ^{1}H NMR ($CDCl_3$): δ 7.83 (d, J = 7.3 Hz, 2H), 7.54–7.41 (m, 4H), 5.89–5.71 (m, 2H), 5.49 (dt, J = 13.9, 7.0 Hz,

1H), 4.61 (m, 2H), 4.33 (m, 1H), 2.99 (m, 3H), 2.41 (m, 3H), 2.18 (m, 2H), 2.06–1.91 (m, 2H). HRMS calcd for $C_{22}H_{26}N_3O_6$ 428.1822, found 428.1803.

5.6.8. (3*S*,6*S*,8*Z*,10a*R*)-*N*-[(3*S*)-2-Hydroxy-5-oxotetrahydrofuran-3-yl]-6-[(2-methoxybenzoyl)amino]-5-oxo-1,2,3,5,6,7,10,10a-octahydropyrrolo[1,2-*a*]azocine-3-carboxamide (17b). ^{1}H NMR ($CDCl_3$): δ 8.84 (d, J = 6.6 Hz, 1H), 8.15 (d, J = 7.5 Hz, 1H), 7.48 (m, 1H), 7.08 (m, 1H), 6.99 (d, J = 8.4 Hz, 1H), 5.98–5.36 (m, 4H), 4.66 (m, 1H), 4.27 (m, 1H), 4.01 (s, 3H), 3.05 (m, 3H), 2.36–1.79 (m, 6H). HRMS calcd for $C_{23}H_{28}N_3O_7$ 458.1927, found 458.1918.

5.6.9. (3*S*,6*S*,8*Z*,10a*R*)-*N*-[(3*S*)-2-Hydroxy-5-oxotetrahydrofuran-3-yl]-6-[(3-methoxybenzoyl)amino]-5-oxo-1,2,3,5,6,7,10,10a-octahydropyrrolo[1,2-*a*]azocine-3-carboxamide (17c). ^{1}H NMR ($CDCl_3$): δ 7.65 (s, 1H), 7.34 (m, 4H), 7.03 (m, 2H), 5.76 (m, 3H), 5.46 (m, 1H), 4.62 (m, 2H), 4.31 (m, 2H), 3.82 (s, 3H), 2.97 (m, 3H), 2.38 (m, 2H), 2.16 (m, 2H), 2.00 (m, 2H). HRMS calcd for $C_{23}H_{28}N_3O_7$ 458.1927, found 458.1905.

5.6.10. (3*S*,6*S*,8*Z*,10a*R*)-*N*-[(3*S*)-2-Hydroxy-5-oxotetrahydrofuran-3-yl]-6-[(4-methoxybenzoyl)amino]-5-oxo-1,2,3,5,6,7,10,10a-octahydropyrrolo[1,2-*a*]azocine-3-carboxamide (17d). ^{1}H NMR ($CDCl_3$): δ 7.80 (d, J = 8.7 Hz, 2H), 7.37 (d, J = 21.0 Hz, 1H), 6.91 (d, J = 8.7 Hz, 2H), 5.86–5.67 (m, 3H), 5.46 (m, 1H), 4.63 (m, 2H), 4.31 (m, 2H), 3.85 (m, 3H), 2.99 (m, 3H), 2.39 (dd, J = 15.0, 7.8 Hz, 2H), 2.28–2.16 (m, 2H), 2.04–1.85 (m, 2H). HRMS calcd for $C_{23}H_{28}N_3O_7$ 458.1927, found 458.1909.

5.6.11. (3*S*,6*S*,8*Z*,10a*R*)-6-[(2-Chlorobenzoyl)amino]-*N*-[(3*S*)-2-hydroxy-5-oxotetrahydrofuran-3-yl]-5-oxo-1,2,3,5,6,7,10,10a-octahydropyrrolo[1,2-*a*]azocine-3-carboxamide (17e). ^{1}H NMR ($CDCl_3$): δ 7.36 (s, 2H), 7.16–7.04 (m, 3H), 5.64–5.42 (m, 3H), 5.27 (m, 1H), 4.39 (s, 2H), 4.08 (s, 2H), 2.81 (m, 3H), 2.57 (m, 2H), 2.21–1.96 (m, 4H), 1.84–1.79 (m, 3H). HRMS calcd for $C_{22}H_{25}N_3O_6Cl$ 462.1432, found 462.1429.

5.6.12. (3*S*,6*S*,8*Z*,10a*R*)-6-[(3-Chlorobenzoyl)amino]-*N*-[(3*S*)-2-hydroxy-5-oxotetrahydrofuran-3-yl]-5-oxo-1,2,3,5,6,7,10,10a-octahydropyrrolo[1,2-*a*]azocine-3-carboxamide (17f). ^{1}H NMR ($CDCl_3$): δ 7.79 (s, 1H), 7.65 (m, 1H), 7.48 (d, J = 8.4 Hz, 1H), 7.73 (m, 2H), 5.87–5.68 (m, 3H), 5.49 (m, 1H), 4.66 (m, 2H), 4.34 (m, 2H), 3.02 (m, 3H), 2.42 (dd, J = 14.7, 8.1 Hz, 2H), 2.33–2.19 (m, 3H), 2.05–1.91 (m, 1H). HRMS calcd for $C_{22}H_{25}N_3O_6Cl$ 462.1432, found 462.1432.

5.6.13. (3*S*,6*S*,8*Z*,10a*R*)-6-[(4-Chlorobenzoyl)amino]-*N*-[(3*S*)-2-hydroxy-5-oxotetrahydrofuran-3-yl]-5-oxo-1,2,3,5,6,7,10,10a-octahydropyrrolo[1,2-*a*]azocine-3-carboxamide (17g). ^{1}H NMR ($CDCl_3$): δ 7.76 (d, J = 8.4 Hz, 2H), 7.41 (d, J = 8.1 Hz, 2H), 7.34 (s, 1H), 6.39 (br s, 1H), 5.87–5.66 (m, 3H), 5.48 (m, 1H), 4.66–4.56 (m, 2H), 4.41–4.32 (m, 2H), 3.01 (m, 3H), 2.44–2.19 (m, 4H), 1.95 (m, 1H). HRMS calcd for $C_{22}H_{25}N_3O_6Cl$ 462.1432, found 462.1411.

5.6.14. (3*S*,6*S*,8*Z*,10a*R*)-*N*-[(3*S*)-2-Hydroxy-5-oxotetrahydrofuran-3-yl]-6-[(2-methylbenzoyl)amino]-5-oxo-1,2,3,5,6,7,10,10a-octahydropyrrolo[1,2-*a*]azocine-3-carboxamide (17h). ^{1}H NMR ($CDCl_3$): δ 7.39–7.30 (m, 3H), 7.22–7.17 (m, 1H), 5.86 (m, 1H), 5.71 (br s, 1H), 5.47 (dt, J = 11.2, 7.0 Hz, 1H), 4.60 (dd, J = 19.0, 6.9 Hz, 1H), 4.33 (m, 1H), 3.09–2.92 (m, 2H), 2.79 (dd, J = 17.2, 8.1 Hz, 1H), 2.38–1.86 (m, 5H). HRMS calcd for $C_{23}H_{28}N_3O_6$ 442.1978, found 442.1970.

5.6.15. (3*S*,6*S*,8*Z*,10a*R*)-*N*-[(3*S*)-2-Hydroxy-5-oxotetrahydrofuran-3-yl]-6-[(3-methylbenzoyl)amino]-5-oxo-1,2,3,5,6,7,10,10a-octahydropyrrolo[1,2-*a*]azocine-3-carboxamide (17i). ^{1}H NMR ($CDCl_3$): δ 7.62–7.58 (m, 2H), 7.32 (m, 3H), 5.89–5.56 (m, 3H), 5.48 (m, 2H), 4.62 (dd, J = 16.9, 7.7 Hz, 2H), 4.34 (m, 1H), 3.01 (m, 2H), 2.83, (dd, J = 16.9, 8.1 Hz, 1H), 2.47–2.16 (m, 3H), 2.38 (s, 3H), 2.00–1.84 (m, 2H). HRMS calcd for $C_{23}H_{28}N_3O_6$ 442.1978, found 442.1967.

5.6.16. (3*S*,6*S*,8*Z*,10a*R*)-*N*-[(3*S*)-2-Hydroxy-5-oxotetrahydrofuran-3-yl]-6-[(4-methylbenzoyl)amino]-5-oxo-1,2,3,5,6,7,10,10a-octahydropyrrolo[1,2-*a*]azocine-3-carboxamide (17j). ^{1}H NMR ($CDCl_3$): δ 7.70 (d, J = 8.0 Hz, 2H), 7.22 (d, J = 8.1 Hz, 2H), 5.89–5.66 (m, 3H), 5.48 (m, 2H), 4.63 (dd, J = 19.7, 8.1 Hz, 2H), 4.35 (m, 1H), 3.01 (m, 2H), 2.82 (dd, J = 17.2, 8.4 Hz, 1H), 2.48–2.18 (m, 3H), 2.39 (s, 3H), 2.00–1.87 (m, 2H). HRMS calcd for $C_{23}H_{28}N_3O_6$ 442.1978, found 442.1969.

5.6.17. (3*S*,6*S*,8*Z*,10a*R*)-6-[(2-Fluorobenzoyl)amino]-*N*-[(3*S*)-2-hydroxy-5-oxotetrahydrofuran-3-yl]-5-oxo-1,2,3,5,6,7,10,10a-octahydropyrrolo[1,2-*a*]azocine-3-carboxamide (17k). ^{1}H NMR ($CDCl_3$): δ 7.85 (dd, J = 8.8, 5.1 Hz, 2H), 7.25–7.11 (m, 3H), 5.91–5.86 (m, 3H), 5.51 (m, 1H), 4.75 (m, 1H), 4.65 (dd, J = 13.6, 8.4 Hz, 1H), 4.32 (m, 1H), 3.06 (m, 2H), 2.87 (dd, J = 17.2, 8.1 Hz, 1H), 2.49–1.84 (m, 6H). HRMS calcd for $C_{22}H_{25}N_3O_6F$ 446.1727, found 446.1715.

5.6.18. (3*S*,6*S*,8*Z*,10a*R*)-6-[(3-Fluorobenzoyl)amino]-*N*-[(3*S*)-2-hydroxy-5-oxotetrahydrofuran-3-yl]-5-oxo-1,2,3,5,6,7,10,10a-octahydropyrrolo[1,2-*a*]azocine-3-carboxamide (17l). ^{1}H NMR ($CDCl_3$): δ 7.56 (dd, J = 12.4, 8.4 Hz, 2H), 7.40 (m, 2H), 7.21 (dt, J = 8.0, 6.3 Hz, 1H), 5.90–5.67 (m, 2H), 5.48 (m, 1H), 4.65 (m, 2H), 4.32 (m, 1H), 3.08–2.97 (m, 2H), 2.83 (dd, J = 17.2, 8.4 Hz, 1H), 2.49–1.84 (m, 6H). HRMS calcd for $C_{22}H_{25}N_3O_6F$ 446.1727, found 446.1713.

5.6.19. (3*S*,6*S*,8*Z*,10a*R*)-6-[(4-Fluorobenzoyl)amino]-*N*-[(3*S*)-2-hydroxy-5-oxotetrahydrofuran-3-yl]-5-oxo-1,2,3,5,6,7,10,10a-octahydropyrrolo[1,2-*a*]azocine-3-carboxamide (17m). ^{1}H NMR ($CDCl_3$): δ 8.00 (t, J = 6.6 Hz, 1H), 7.65 (m, 1H), 7.49 (m, 1H), 7.26 (m, 1H), 7.14 (dd, J = 11.7, 8.4 Hz, 1H), 5.91–5.68 (m, 3H), 5.51 (m, 1H), 4.66 (m, 2H), 4.29 (m, 1H), 3.06 (m, 2H), 2.83 (dd, J = 16.8, 8.4 Hz, 1H), 2.49–2.17 (m, 3H), 2.05–1.85 (m, 2H). HRMS calcd for $C_{22}H_{25}N_3O_6F$ 446.1727, found 446.1729.

5.6.20. (3*S*,6*S*,8*Z*,10a*R*)-*N*-[(3*S*)-2-Hydroxy-5-oxotetrahydrofuran-3-yl]-5-oxo-6-{[2-(trifluoromethyl)benzoyl]amino}-1,2,3,5,6,7,10,10a-octahydropyrrolo[1,2-*a*]azocine-3-carboxamide (17n). ^{1}H NMR ($CDCl_3$): δ 7.71 (d, J = 7.4 Hz, 1H), 7.58 (m, 3H), 7.25 (br s, 1H), 7.11 (br s, 1H), 5.86–5.73 (m, 3H), 5.46 (m, 1H), 4.58–4.49 (m, 1H), 4.29 (br s, 1H), 3.01 (m, 2H), 2.78 (dd, J = 13.9, 6.6 Hz, 1H), 2.42–2.08 (m, 5H), 2.04–1.85 (m, 2H). HRMS calcd for $C_{23}H_{25}N_3O_6F_3$ 496.1695, found 496.1695.

5.6.21. (3*S*,6*S*,8*Z*,10a*R*)-*N*-[(3*S*)-2-Hydroxy-5-oxotetrahydrofuran-3-yl]-5-oxo-6-{[3-(trifluoromethyl)benzoyl]amino}-1,2,3,5,6,7,10,10a-octahydropyrrolo[1,2-*a*]azocine-3-carboxamide (17o). ^{1}H NMR ($CDCl_3$): δ 8.11–7.92 (m, 2H), 7.79 (m, 1H), 7.55 (m, 1H), 7.49–7.37 (m, 1H), 5.92–5.71 (m, 2H), 5.55 (m, 1H), 4.63 (m, 1H), 4.39 (s, 1H), 3.09–2.92 (m, 3H), 2.43 (m, 2H), 2.22 (m, 2H), 2.11–1.85 (m, 2H). HRMS calcd for $C_{23}H_{25}N_3O_6F_3$ 496.1695, found 496.1694.

5.6.22. (3*S*,6*S*,8*Z*,10a*R*)-*N*-[(3*S*)-2-Hydroxy-5-oxotetrahydrofuran-3-yl]-5-oxo-6-{[2-(trifluoromethyl)benzoyl]amino}-1,2,3,5,6,7,10,10a-octahydropyrrolo[1,2-*a*]azocine-3-carboxamide (17p). ^{1}H NMR ($CDCl_3$): δ 7.70 (d, J = 7.4 Hz, 1H), 7.61–7.51 (m, 3H), 7.09 (br s, 1H), 5.85 (m, 2H), 5.74 (m, 1H), 5.50 (m, 1H), 4.58 (m, 1H), 4.31 (m, 1H), 3.03 (m, 2H), 2.80 (dd, J = 17.1, 8.1 Hz, 1H), 2.40 (dd, J = 14.7, 8.1 Hz, 1H), 2.18 (m, 3H), 2.04–1.83 (m, 2H). HRMS calcd for $C_{23}H_{25}N_3O_6F_3$ 496.1695, found 496.1716.

5.6.23. (3*S*,6*S*,8*Z*,10a*R*)-6-[(1-Benzothien-2-yl-carbonyl)amino]-*N*-[(3*S*)-2-hydroxy-5-oxotetrahydrofuran-3-yl]-5-oxo-1,2,3,5,6,7,10,10a-octahydropyrrolo[1,2-*a*]azocine-3-carboxamide (17q). ^{1}H NMR ($CDCl_3$): δ 7.95–7.80 (m, 3H), 7.42 (m, 3H), 7.26–7.13 (m, 1H), 5.85–5.17 (m, 5H), 4.64–4.28 (m, 3H), 3.21–2.76 (m, 4H), 2.54 (m,1H), 2.41–1.66 (m, 8H). HRMS calcd for $C_{24}H_{26}N_3O_6S$ 484.1542, found 484.1533.

5.6.24. (3*S*,6*S*,8*Z*,10a*R*)-*N*-[(3*S*)-2-Hydroxy-5-oxotetrahydrofuran-3-yl]-6-(1-naphthoylamino)-5-oxo-1,2,3,5,6,7,10,10a-octahydropyrrolo[1,2-*a*]azocine-3-carboxamide (17r). ^{1}H NMR (CD_3OD): δ 8.78 (m, 1H), 8.29 (d, J = 6.0 Hz, 1H), 8.01 (d, J = 8.4 Hz, 1H), 7.94 (m, 1H), 7.71 (m, 1H), 7.57 (m, 2H), 6.03 (m, 2H), 5.51 (m, 1H), 4.57 (m, 2H), 4.42 (m, 2H), 3.20–2.95 (m, 2H), 2.77–2.65 (m, 1H), 2.58–2.40 (m, 3H), 2.23–1.88 (m, 5H). HRMS calcd for $C_{26}H_{28}N_3O_6$ 478.1978, found 478.1961.

5.6.25. (3*S*,6*S*,8*Z*,10a*R*)-*N*-[(3*S*)-2-Hydroxy-5-oxotetrahydrofuran-3-yl]-6-(2-naphthoylamino)-5-oxo-1,2,3,5,6,7,10,10a-octahydropyrrolo[1,2-*a*]azocine-3-carboxamide (17s). ^{1}H NMR ($CDCl_3$): δ 8.34 (s, 1H), 7.93–7.83 (m, 4H), 7.66–7.51 (m, 3H), 7.42 (s, 1H), 5.90–5.70 (m, 2H), 5.53 (m, 1H), 4.59 (m, 2H), 4.28 (m, 1H), 2.96 (m, 3H), 2.38 (m, 2H), 2.15 (m, 2H), 2.02–1.79 (m, 3H). ^{13}C NMR ($CDCl_3$): δ 176.1, 173.1, 171.6, 167.8, 135.3, 132.9, 130.6, 129.5, 128.8, 128.5, 128.3, 128.1, 127.2, 125.9, 124.0, 61.9, 59.1, 50.9, 33.9, 33.5, 32.3, 27.1, 21.1. HRMS calcd for $C_{26}H_{28}N_3O_6$ 478.1978, found 478.1970.

5.6.26. (3*S*,6*S*,8*Z*,10a*R*)-*N*-[(3*S*)-2-Hydroxy-5-oxotetrahydrofuran-3-yl]-5-oxo-6-{[(2E)-3-phenylprop-2-enoyl]amino}-1,2,3,5,6,7,10,10a-octahydropyrrolo[1,2-*a*]azocine-3-carboxamide (17u). ^{1}H NMR ($CDCl_3$): δ 7.76–7.31 (m, 7H), 7.07 (m, 1H), 6.69–6.44 (m, 1H), 5.89–5.67 (m, 2H), 5.49 (m, 1H), 4.68 (m, 2H), 4.49–4.24 (m, 1H), 3.12–2.91 (m, 4H), 2.54–1.85 (m, 6H). HRMS calcd for $C_{24}H_{28}N_3O_6$ 454.1978, found 454.1985.

5.6.27. (3*S*,6*S*,10a*S*)-6-(Benzoylamino)-*N*-[(3*S*)-2-hydroxy-5-oxotetrahydrofuran-3-yl]-5-oxodecahydropyrrolo[1,2-*a*]azocine-3-carboxamide (18a). ^{1}H NMR ($CDCl_3$): δ 8.05–7.65 (m, 3H), 7.60–7.46 (m, 3H), 5.70 (br s, 1H), 5.11 (br s, 1H), 4.62–4.27 (m, 3H), 3.01 (m, 4H), 2.21–1.68 (m, 11H). HRMS calcd for $C_{22}H_{28}N_3O_6$ 430.1978, found 430.1969.

5.6.28. (3*S*,6*S*,10a*S*)-6-[(2-Chlorobenzoyl)amino]-*N*-[(3*S*)-2-hydroxy-5-oxotetrahydrofuran-3-yl]-5-oxodecahydropyrrolo[1,2-*a*]azocine-3-carboxamide (18e). ^{1}H NMR (CD_3OD): δ 7.56–7.37 (m, 4H), 5.05 (m, 1H), 4.64 (m, 1H), 4.52–4.22 (m, 4H), 2.75–2.62 (m, 1H), 2.60–2.44 (m, 1H), 2.21 (m, 3H), 2.10–1.60 (m, 12H). HRMS calcd for $C_{22}H_{27}N_3O_6Cl$ 464.1588, found 464.1607.

5.6.29. (3*S*,6*S*,10a*S*)-6-[(3-Chlorobenzoyl)amino]-*N*-[(3*S*)-2-hydroxy-5-oxotetrahydrofuran-3-yl]-5-oxodecahydropyrrolo[1,2-*a*]azocine-3-carboxamide (18f). ^{1}H NMR (CD_3OD): δ 7.91 (t, J = 2.1 Hz, 1H), 7.82 (m, 1H), 7.57 (m, 1H), 7.48 (m, 1H), 5.04 (m, 1H), 4.65 (m, 1H), 4.50–4.26 (m, 4H), 2.69–2.52 (m, 2H), 2.22 (m, 3H), 2.05–1.62 (m, 11H). HRMS calcd for $C_{22}H_{27}N_3O_6Cl$ 464.1588, found 464.1590.

5.6.30. (3*S*,6*S*,10a*S*)-6-[(4-Chlorobenzoyl)amino]-*N*-[(3*S*)-2-hydroxy-5-oxotetrahydrofuran-3-yl]-5-oxodecahydropyrrolo[1,2-*a*]azocine-3-carboxamide (18g). ^{1}H NMR (CD_3OD): δ 7.87 (d, J = 8.4 Hz, 2H), 7.49 (d, J = 8.4 Hz, 2H), 5.03 (m, 1H), 4.65 (m, 1H), 4.52–4.38 (m, 3H), 4.35–4.25 (m, 1H), 2.70–2.50 (m, 2H), 2.25–2.16 (m, 3H), 2.01–1.58 (m, 11H). HRMS calcd for $C_{22}H_{27}N_3O_6Cl$ 464.1588, found 464.1587.

5.6.31. (3*S*,6*S*,10a*S*)-6-[(1-Benzothien-2-ylcarbonyl)amino]-*N*-[(3*S*)-2-hydroxy-5-oxotetrahydrofuran-3-yl]-5-oxodecahydropyrrolo[1,2-*a*]azocine-3-carboxamide (18q). ^{1}H NMR ($CDCl_3$): δ 7.87 (m, 3H), 7.43 (m, 2H), 5.14 (m, 1H), 4.63 (m, 1H), 4.34–4.17 (m, 2H), 2.52 (q, J = 7.6 Hz, 1H), 2.39–1.62 (m, 8H), 1.36 (m, 3H). HRMS calcd for $C_{24}H_{28}N_3O_6S$ 486.1699, found 486.1718.

5.6.32. (3*S*,6*S*,10a*S*)-*N*-[(3*S*)-2-Hydroxy-5-oxotetrahydrofuran-3-yl]-6-(1-naphthoylamino)-5-oxodecahydropyrrolo[1,2-*a*]azocine-3-carboxamide (18r). ^{1}H NMR (CD_3OD): δ 8.86 (m, 1H), 8.29 (m, 1H), 8.00 (d, J = 7.8 Hz, 1H), 7.93 (m, 1H), 7.70 (m, 1H), 7.58–7.51 (m, 3H), 5.13 (m 1H), 4.66 (m, 1H), 4.60–4.43 (m, 2H), 4.30 (m, 1H), 2.68–2.55 (m, 1H), 2.35–2.19 (m, 2H), 2.11–1.70 (m, 9H). HRMS calcd for $C_{26}H_{30}N_3O_6$ 480.2135, found 480.2137.

5.6.33. (3*S*,6*S*,10a*S*)-*N*-[(3*S*)-2-Hydroxy-5-oxotetrahydrofuran-3-yl]-6-(1-naphthoylamino)-5-oxodecahydropyrrolo[1,2-*a*]azocine-3-carboxamide (18s). ^{1}H NMR ($CDCl_3$): δ 8.37 (br s, 1H), 7.96–7.86 (m,4H), 7.57–7.47 (m, 3H), 7.11 (d, J = 5.1 Hz, 1H), 5.78 (m, 1H), 5.16 (m, 1H), 4.79–4.48 (m, 1H), 4.64–4.35 (m, 2H), 3.10–2.75 (m, 2H), 2.56–1.62 (m, 12H). HRMS calcd for $C_{26}H_{30}N_3O_6$ 480.2135, found 480.2125.

5.6.34. (3*S*,6*S*,10a*S*)-6-[(2,6-Dimethylbenzoyl)amino]-*N*-[(3*S*)-2-hydroxy-5-oxotetrahydrofuran-3-yl]-5-oxodecahydropyrrolo[1,2-*a*]azocine-3-carboxamide (18v). ^{1}H NMR ($CDCl_3$): δ 7.16 (m, 1H), 7.01 (m, 2H), 5.80–5.60 (m, 2H), 5.18 (m, 2H), 4.61–4.22 (m, 2H), 3.01–2.63 (m, 1H), 2.28 (s, 6H), 2.22–1.95 (m, 1H), 1.88–1.52 (m, 10H). HRMS calcd for $C_{24}H_{32}N_3O_6$ 458.2291, found 458.2275.

5.6.35. (3*S*,6*S*,8*Z*,10a*S*)-6-(benzoylamino)-*N*-[(3*S*)-2-hydroxy-5-oxotetrahydrofuran-3-yl]-5-oxo-1,2,3,5,6,7,10,10a-octahydropyrrolo[1,2-*a*]azocine-3-carboxamide (19a). ^{1}H NMR ($CDCl_3$): δ 7.76 (m, 2H), 7.55–7.30 (m, 3H), 5.93–5.64 (m, 2H), 5.48 (m, 1H), 4.91 (br s, 1H), 4.66 (m, 2H), 4.29 (m, 1H), 3.17–2.82 (m,3H), 2.52–1.91 (m, 6H). HRMS calcd for $C_{22}H_{26}N_3O_6$ 428.1822, found 428.1831.

5.6.36. (3*S*,6*S*,8*Z*,10a*S*)-*N*-[(3*S*)-2-Hydroxy-5-oxotetrahydrofuran-3-yl]-6-[(3-methoxybenzoyl)amino]-5-oxo-1,2,3,5,6,7,10,10a-octahydropyrrolo[1,2-*a*]azocine-3-carboxamide (19c). ^{1}H NMR ($CDCl_3$): δ 7.34 (m, 4H), 7.05 (m, 1H), 6.03–5.46 (m, 4H), 4.61 (m, 2H), 4.31 (m, 2H), 3.83 (s, 3H), 2.98 (m, 4H), 2.35 (m, 2H), 2.16 (m, 2H), 1.97 (m, 2H). HRMS calcd for $C_{23}H_{28}N_3O_7$ 458.1927, found 458.1928.

5.6.37. (3*S*,6*S*,8*Z*,10a*S*)-*N*-[(3*S*)-2-Hydroxy-5-oxotetrahydrofuran-3-yl]-6-[(isoquinolin-1-ylcarbonyl)amino]-5-oxo- 1,2,3,5,6,7,10,10a-octahydropyrrolo[1,2-*a*]azocine-3-carboxamide (19t). ^{1}H NMR ($CDCl_3$): δ 9.37 (br s, 1H), 8.87 (d, J = 6.9 Hz, 1H), 8.47 (s, 1H), 7.86–7.65 (m, 4H), 7.55–7.41 (m, 1H), 6.56 (br s, 1H), 5.97–5.70 (m, 3H), 5.50 (m, 3H), 5.50 (m, 1H), 4.66 (d, J = 6.9 Hz, 2H), 4.32 (br s, 2H), 3.03–2.74 (m, 4H), 2.43 (m, 3H), 2.18 (m, 2H), 1.98 (m, 2H). HRMS calcd for $C_{25}H_{27}N_4O_6$ 479.1931, found 479.1929.

5.6.38. (3*S*,6*S*,10a*R*)-6-(Benzoylamino)-*N*-[(3*S*)-2-hydroxy-5-oxotetrahydrofuran-3-yl]-5-oxodecahydropyrrolo-[1,2-*a*]azocine-3-carboxamide (20a). ^{1}H NMR ($CDCl_3$): δ 7.68 (m, 2H), 7.54–7.23 (m, 4H), 5.03 (br s, 1H), 4.76–4.42 (m, 1H), 4.35 (m, 2H), 2.91–2.64 (m, 3H), 2.48 (m, 3H), 2.28–1.41 (m, 10H). HRMS calcd for $C_{22}H_{28}N_3O_6$ 430.1978, found 430.1995.

5.6.39. (3*S*,6*S*,10a*R*)-*N*-[(3*S*)-2-Hydroxy-5-oxotetrahydrofuran-3-yl]-6-[(3-methoxybenzoyl)amino]-5-oxodecahydropyrrolo[1,2-*a*]azocine-3-carboxamide (20c). ^{1}H NMR ($CDCl_3$): δ 7.39–7.28 (m, 3H), 7.02 (d, J = 7.7 Hz, 1H), 5.32 (d, J = 2.5 Hz, 1H), 5.08 (m, 1H), 4.34 (m, 1H), 4.17–4.05 (m, 1H), 3.82 (s, 3H), 2.89 (m, 1H), 2.51 (q, J = 7.6 Hz, 1H), 2.34–0.85 (m, 15H). HRMS calcd for $C_{23}H_{30}N_3O_7$ 460.2084, found 430.2083.

5.6.40. (3*S*,6*S*,10a*R*)-*N*-[(3*S*)-2-Hydroxy-5-oxotetrahydrofuran-3-yl]-6-[(isoquinolin-1-ylcarbonyl)amino]-5-oxodecahydropyrrolo[1,2-*a*]azocine-3-carboxamide (20t). ^{1}H NMR ($CDCl_3$): δ 9.37 (d, J = 7.6 Hz, 1H), 8.82–8.74 (m, 1H), 8.48 (t, J = 4.4 Hz, 1H), 7.81 (m, 2H), 7.69 (m, 3H), 5.15 (br s, 1H), 4.37 (m, 1H), 4.13 (m, 1H), 2.51 (q, J = 7.6 Hz, 1H), 2.32 (m, 1H), 2.18–1.58 (m, 11H), 1.27 (m, 6H), 1.01–0.82 (m, 3H). HRMS calcd for $C_{25}H_{29}N_4O_6$ 481.2087, found 481.2101.

Acknowledgments

We thank Mr. Brian Regg for performing the HRMS analyses, Ms. Anne Russell for performing the 2D NOESY NMR experiment with compound **12**, and Dr. Greg Bosch and Ms. Kenetha Stanton for providing quantities of intermediates **21** and **22**.

References and notes

1. (a) Dinarello, C. A.; Wolff, S. M. *N. Engl. J. Med.* **1993**, *328*, 106; (b) Goldring, M. B. *Exp. Opin. Biol. Ther.* **2001**, *1*, 817; (c) Malemud, C. J. *BioDrugs* **2004**, *18*, 23.
2. (a) Wei, Y.; Fox, T.; Chambers, S. P.; Sintchak, J.; Coll, J. T.; Golec, J. M. C.; Swenson, L.; Wilson, K. P.; Charifson, P. S. *Chem. Biol.* **2000**, *7*, 423; (b) Alnemri, E. S.; Livingston, D. J.; Nicholson, D. W.; Salvesen, G.; Thornberry, N. A.; Wong, W. W.; Yuan, J. *Cell* **1996**, *87*, 171.
3. (a) Kostura, M. J.; Tocci, M. J.; Limjuco, G.; Chin, J.; Cameron, P.; Hillman, A. G.; Chartrain, N. A.; Schmidt, J. A. *Proc. Natl. Acad. Sci. U.S.A.* **1989**, *86*, 5227; (b) Black, R. A.; Kronheim, S. R.; Cantrell, M.; Deeley, M. C.; March, C. J.; Prickett, K. S.; Wignall, J.; Conlon, P. J.; Cosman, D.; Hopp, T. P.; Mochizuki, D. Y. *J. Biol. Chem.* **1988**, *263*, 9437.
4. Chapman, K. T. *Bioorg. Med. Chem. Lett.* **1992**, *2*, 613.
5. For reviews of caspase-1 inhibitors, see (a) Talanian, R. V.; Brady, K. D.; Cryns, V. L. *J. Med. Chem.* **2000**, *43*, 3351; (b) Ashwell, S. *Exp. Opin. Ther. Patents* **2001**, *11*, 1593.
6. Wilson, K. P.; Black, J. F.; Thomson, J. T.; Kim, E. K.; Griffith, J. P.; Navia, M. N.; Murcko, M. A.; Chambers, S. P.; Aldape, R. A.; Raybuck, S. A.; Livingston, D. J. *Nature* **1994**, *370*, 270.
7. Thornberry, N. A.; Bull, H. G.; Calaycay, J. R.; Chapman, K. T.; Howard, A. D.; Kostura, M. J.; Miller, D. K.; Molieaux, S. M.; Weidner, J. R.; Aunins, J.; Elliston, K. O.; Ayala, J. M.; Casano, F. J.; Chin, J.; Ding, G. J.-F.; Egger, L. A.; Gaffney, E. P.; Limjuco, G.; Palyha, O. C.; Raju, S. M.; Rolando, A. M.; Salley, J. P.; Yamin, T-T.; Lee, T. D.; Shively, J. E.; MacCross, M.; Mumford, R. A.; Schmidt, J. A.; Tocci, M. J. *Nature* **1992**, *356*, 786.
8. Dolle, R. E.; Prasad, C. V. C.; Prouty, C. P.; Salvino, J. M.; Awad, M. M. A.; Schmidt, S. J.; Hoyer, D.; Ross, T. M.; Graybill, T. L.; Speier, G. J.; Uhl, J.; Miller, B. E.; Helaszek, C. T.; Ator, M. A. *J. Med. Chem.* **1997**, *40*, 1941.
9. Rudolphi, K.; Gerwin, N.; Verzijl, N.; van der Kraan, P.; van den Berg, W. *OsteoArthritis Cartilage* **2003**, *11*, 738.
10. (a) O'Neil, S. V.; Wang, Y.; Laufersweiler, M. C.; Oppong, K. A.; Soper, D. L.; Wos, J. A.; Ellis, C. D.; Baize, M. W.; Bosch, G. K.; Fancher, A. N.; Lu, W.; Suchanek, M. K.; Wang, R. L.; De, B.; Demuth, T. P., Jr. *Bioorg. Med. Chem. Lett.* **2005**, *15*, 5434; (b)

Laufersweiler, M. C.; Wang, Y.; Soper, D. L.; Suchanek, M. K.; Fancher, A. N.; Lu, W.; Wang, R. L.; Oppong, K. A.; Ellis, C. D.; Baize, M. W.; O'Neil, S. V.; Wos, J. A.; Demuth, T. P., Jr. *Bioorg. Med. Chem. Lett.* **2005**, *15*, 4322.

11. (a) Grossmith, C. E.; Senia, F.; Wagner, J. *Synlett* **1999**, *10*, 1660–1662; (b) Harris, P. W. R.; Brimble, M. A.; Gluckman, P. D. . *Org. Lett.* **2003**, *5*, 1847–1850.
12. Schwab, P.; France, M. B.; Ziller, J. W.; Grubbs, R. H. *Angew. Chem., Int. Ed. Engl.* **1995**, *34*, 2039.
13. (a) Tang, H.; Yusuff, N.; Wood, J. L. *Org. Lett.* **2001**, *3*, 1563; (b) Kigoshi, H.; Suzuki, Y.; Aoki, K.; Uemura, D. *Tetrahedron Lett.* **2000**, *41*, 3927.
14. (a) Seeman, J. I. *Chem. Rev.* **1983**, *83*, 83; (b) Smith, A. B., III; Mesaros, E. F.; Meyer, E. A. *J. Am. Chem. Soc.* **2006**, *128*, 5292.
15. (a) Batchelor, M. J.; Bebbington, D.; Bemis, G. W.; Fridman, W. H.; Gillespie, R. J.; Golec, J. M. C.; Gu, Y.; Lauffer, D. J.; Livingston, D. J.; Matharu, S. S.; Mullican, M. D.; Murcko, M. A.; Murdoch, R.; Nyce, P. L.; Robidoux, A. L. C.; Su, M.; Wannamaker, M.; Wilson, K. P.; Zelle, R. E. WO 97/22619, 1997; (b) Wos, J. A.; Soper, D. L.; O'Neil, S. V.; Wang, Y.; Oppong, K. A.; Laufersweiler, M. C.; Chen, J.; De, B.; Demuth, T. P., Jr. WO 2003/106460, 2003.
16. Crystallographic data (excluding structure factors) for compound **13f** were deposited with the Cambridge Crystallographic Data Centre as supplementary Publication No. CCDC 608956. Copies of the data can be obtained, free of charge, on application to CCDC, 12 Union Road, Cambridge CB2 1EZ, UK (fax: +44 (0) 1223 336033 or e-mail:deposit@ccdc.cam.ac.uk).
17. Non-GLP pharmacokinetic analyses were conducted using male Sprague–Dawley rats (2–4 animals/group) with oral gavage administration. Plasma samples were prepared by protein precipitation with acetonitrile. Drug levels were monitored over 24 h using reverse-phase HPLC/MS/MS. Pharmacokinetic parameters, including plasma half-life and % oral bioavailability, were calculated using the group-averaged time/concentration values.
18. (a) Halgren, T. A. *J. Comput. Chem.* **1996**, *17*, 490; (b) Halgren, T. A. *J. Comput. Chem.* **1996**, *17*, 520; (c) Halgren, T. A. *J. Comput. Chem.* **1996**, *17*, 553; (d) Halgren, T. A. *J. Comput. Chem.* **1996**, *17*, 587; (e) Halgren, T. A. *J. Comput. Chem.* **1996**, *17*, 616.
19. MacroModel 7.0, Schrodinger Inc. 2000.
20. (a) Hasel, W.; Hendrickson, T. F.; Still, W. C. *Tetrahedron Comput. Method* **1988**, *1*, 103; (b) Still, W. C.; Tempczyk, A.; Hawley, R. C.; Hendrickson, T. *J. Am. Chem. Soc.* **1990**, *112*, 6127.